ADVANCED NANOBIOMED RESEARCH Open Access
www.advnanobiomedres.com

Microfluidic Encapsulation of DNAs in Liquid Beads for Digital Loop-Mediated Isothermal Amplification

*Fariba Malekpour Galogahi, Simon Strachan, Ajeet Singh Yadav, Helen Stratton, and Nam-Trung Nguyen**

Digital nucleic acid analysis has emerged as a prominent tool for the detection and absolute quantification of diverse pathogens. Digital loop-mediated isothermal amplification (dLAMP) offers highly sensitive, specific, time-efficient, and cost-effective nucleic acid amplification. However, existing dLAMP techniques face challenges such as droplet merging, reliance on surfactants, restricted partition capacities, and the potential for sample loss during heating. Herein, these issues are addressed by introducing liquid beads for sample partitioning. Compared to microwells, our approach overcomes the limitations of chamber dimensions, enabling the analysis of an unlimited number of digitized targets. Furthermore, our novel approach effectively addresses sample loss and merging during thermal processing and eliminates the need for surfactants. Accurate and reproducible the quantitative detection of the gene cluster XALB1 of leaf scald disease is conducted using dLAMP based on liquid beads to verify its availability. The results demonstrate a high correlation between target concentration and positive signals, indicating the robust performance of our technique. A comparative analysis is then performed between dLAMP using liquid beads and using single droplets. Benchmarking these two techniques highlights the effectiveness of our innovative technique in overcoming existing challenges in dLAMP.

1. Introduction

Nucleic acid analysis has emerged as the preferred method for highly sensitive detection and precise quantification of various DNA or RNA molecules within biological samples. However, the limited quantity of target DNA or RNA molecules often makes direct detection challenging. Hence, in most nucleic acid analysis, it is crucial to amplify these molecules to a detectable level.[1] Among the various nucleic acid amplification techniques available, polymerase chain reaction (PCR) stands out as the most commonly used. PCR facilitates exponential amplification of nucleic acid molecules through primer-initiated reactions via thermocycling.[2] However, PCR has drawbacks that can restrict its application. A notable limitation is its reliance on time-consuming thermal cycling, lasting over an hour and necessitating costly equipment for precise temperature control.[2] Attempts to accelerate thermal cycling using rapid cycling instruments have been reported, but this may compromise the sensitivity and reproducibility of specific tests.[3] Quantitative PCR (qPCR), recognized for its high sensitivity, is limited by its dependence on cycle threshold (Ct) measurements, providing only relative quantification.[4] Moreover, real-time PCR requires advanced facilities for sample processing. It usually demands at least 2–4 h to yield outcomes.[5] To address these challenges, loop-mediated isothermal amplification (LAMP) emerges as a promising alternative. LAMP provides enhanced specificity through the utilization of multiple primer sets targeting a single gene compared to traditional PCR. LAMP eliminates the need for expensive thermal cyclers and allows for absolute quantification of targets without the requirement for calibrants or standard curves.[1] Moreover, LAMP demonstrates notable time efficiency, typically completing in less than one hour.[6]

Nucleic acid detection has found widespread application across various fields, such as biotechnology, genetic engineering, and environmental monitoring. The significance of nucleic acid detection tests becomes particularly evident during human and environmental disease outbreaks caused by bacteria and viruses, emphasizing their crucial role in pandemic and epidemic management. In agriculture, the significance and necessity of this technique have been well exemplified by the leaf scald disease outbreak, establishing it as the pioneering technique for highly precise detection and differentiation of pathogens.[7] Infected plants may remain asymptomatic during the latency stage for several months.[8] This silent period allows pathogenic bacteria to proliferate and spread across sugarcane fields undetected during the early phases of the plant's growth cycle.[9] Therefore, the early and precise identification of the pathogen during asymptomatic stage is crucial. This is not only for effectively containing

F. M. Galogahi, S. Strachan, A. S. Yadav, H. Stratton, N.-T. Nguyen
Queensland Micro- and Nanotechnology Centre
Griffith University
170 Kessels Road, Nathan, Queensland 4111, Australia
E-mail: nam-trung.nguyen@griffith.edu.au

The ORCID identification number(s) for the author(s) of this article can be found under https://doi.org/10.1002/anbr.202400044.

DOI: 10.1002/anbr.202400044

its distribution but also for facilitating the genetic improvement of sugarcane.[10] Nucleic acid-based methods, including PCR and LAMP, have revolutionized the detection of sugarcane pathogenic diseases, playing a crucial role in managing these disease outbreaks. These techniques offer exceptional sensitivity and have fewer detection limitations compared to traditional methods.[11–13] However, their effectiveness can be compromised when the target concentration is extremely low. For instance, detecting pathogens in asymptomatic leaves, where the pathogen population is very low and nonuniformly distributed within the plant, presents a significant challenge.[10] Additionally, these methods lack the capacity for visual determination of end-point results, which can pose a limitation in certain diagnostic contexts.[2]

To address these limitations in traditional PCR and LAMP methods, innovative digital nucleic acid amplification techniques have been developed. Digital amplification techniques emerge as a promising alternative for achieving enhanced sensitivity, reaching as low as 0.5 copies μL^{-1}.[13] When comparing digital LAMP (dLAMP) to digital PCR (dPCR), dLAMP retains all the advantages of traditional LAMP over traditional PCR. In this method, a minute microliter-sized sample is rapidly partitioned into thousands of tiny picolitre compartments. Each individual partition functions as an independent reactor for the amplification process, encapsulating either zero or one target molecule.[14] Following amplification, quantification of target molecules is achieved by counting the number of partitions displaying positive fluorescent signals. The quantification relies on the analysis of Poisson statistics, which is based on the ratio of fluorescent to nonfluorescent droplets.[15] Various techniques have been devised for sample compartmentalization, including microwells, microfluidic chambers, and droplets.[16,17] Microwells or chips pose certain limitations, such as a limited number of micropartitions, inconsistent partition volumes, and the possibility of cross contamination.[17] The size of samples in microwell techniques may be influenced by the interfacial tension and viscosity of the oil, leading to a nonuniform size distribution that can impact accuracy.[1] In contrast, droplet-based technology employs microfluidics to ensure consistent droplet sizes. A key advantage of droplet-based microfluidics is the significant reduction in the consumption of reaction reagents, thereby enhancing cost-efficiency.[18] Furthermore, microfluidic devices provide a high degree of precision and control over the conditions of droplet generation and the size of the droplets.[19,20] Microfluidics-based nucleic acid amplification opens the possibility for fully automated testing within enclosed systems, enabling sample-in, answer-out capabilities for rapid nucleic acid diagnostics.[21] Moreover, microfluidic platforms can be integrated with off-chip sample processing steps prior to loading, enhancing the overall efficiency of the testing process.[22] Despite the numerous advantages of digital technology, there are still some limitations that need to be addressed. One issue is the possible merging of droplets during droplet transfer and thermal cycling, which can affect the quantification accuracy.[23] Another limitation is the edge effects during PCR due to thermal motion or the evaporation of the continuous phase. Additionally, there can be compatibility issues between the master mixture and the oil continuous phase. Furthermore, there is a risk of sample evaporation that needs to be considered.[24] Another key drawback is the limited scalability, as the production and precise handling of large numbers of uniform droplets require sophisticated microfluidic setups and are prone to technical bottlenecks.

Core–shell particles can provide an effective solution for addressing these challenges. Despite the increased complexity involved in generating core–shell structures compared to single droplets, they offer distinct advantages. Each solid shell provides specific protection against evaporation and droplet merging, while also preventing cross contamination. Core–shell particles offer a consistent particle size, eliminating concerns about partition size variability.[25] In core–shell particle-based digital amplification, there is no limitation on the number of wells and partitions.[26] An unlimited number of particles can be generated and collected in various plates as needed, offering unparalleled flexibility and scalability in experimental design and sample processing. These particles are easily transferable to various plates and containers. The transparent shells facilitate the straightforward detection of fluorescent signals. A key advantage of the protective shell structure is its ability to offer thermal and mechanical stability, enabling these liquid beads to be utilized in applications where genome amplification is required after specific processing steps. For example, core–shell structures have the potential to act as biological tracers for studying flow paths and contaminant migration in environments like air, rivers, and food products. Moreover, core–shell structures can be employed for single-cell encapsulation, enabling downstream genome amplification and analysis, thus expanding the capabilities of single-cell genomics and environmental monitoring. Despite the increased complexity of generating core–shell structures, their advantages may outweigh those of single droplets in niche applications.

In pursuit of this objective, our team employed a simple and cost-effective microfluidic device, eschewing the need for a specially designed collection chamber, to produce liquid beads with an aqueous core. The device features high-density partitioning, ensuring a user-friendly workflow with remarkable high-throughput capabilities. The device demonstrated the capability to generate uniformly sized genetic mixture droplets, each of which could be individually encapsulated within a distinct shell. The resulting particles had a transparent shell, facilitating the observation of fluorescent signals. Despite the abundant recent literature on dLAMP using microfluidic single droplets, to the best of our knowledge, there is no report on the application of liquid beads for dLAMP. As a proof of concept, we demonstrate the quantification of the gene cluster XALB1 using liquid bead-based dLAMP (**Figure 1**). To comprehensively compare the advantages of the liquid beads, we also conducted dLAMP with single droplets using the same device design and experimental conditions. Our results demonstrate the capability of absolute quantification of template numbers through liquid bead-based dLAMP.

2. Results and Discussion

All the key advantage of microfluidics-based nucleic acid amplification lies in its ability to produce homogeneous partitions with high throughput. Therefore, precise control over partition size and monodispersity is essential. Existing digital nucleic acid

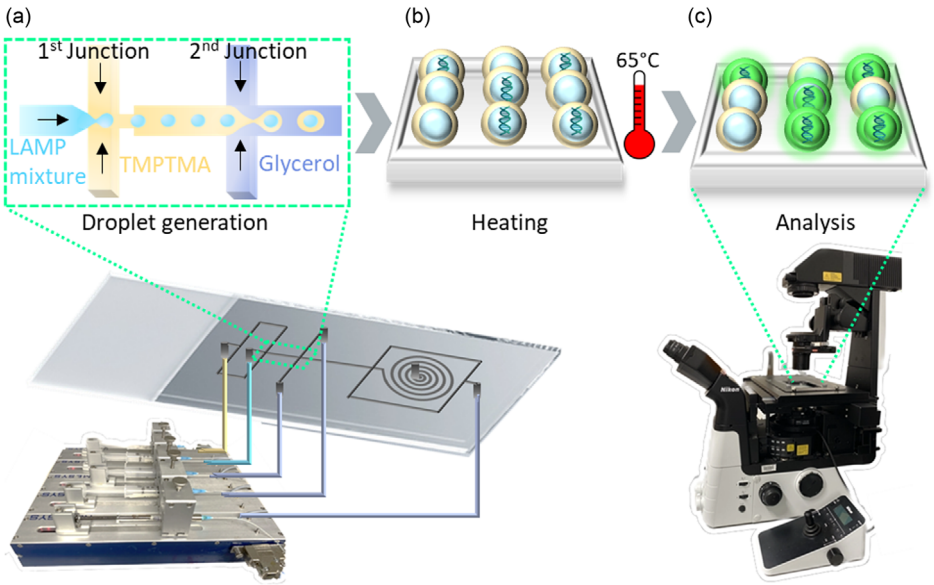

Figure 1. Digital loop-mediated isothermal amplification with liquid beads: a) microfluidic setup for the generation of liquid beads, b) Heating, and c) Analysis.

amplification systems have inherent limitations. The reaction mixture undergoes evaporation during the amplification process. Droplet coalescence might occur during the thermocycling process, necessitating the use of surfactants. The concentration of surfactant is a critical determinant of droplet stability. Low surfactant concentration can lead to droplet merging, while excessive concentrations can cause droplet dissolution within the oil phase or disrupt the DNA amplification. In various techniques, droplets are collected into a PCR tube for amplification and then transferred to a specialized platform for signal analysis. A considerable number of samples may be lost during the transformation process, subsequently leading to decreased accuracy. Recent efforts have focused on designing a microfluidic device with an integrated collection chamber, eliminating the need for droplet transfer. However, due to the porosity and hydrophobicity of PDMS, a significant quantity of the oil used as the continuous phase can be absorbed into the PDMS under heat. This absorption may lead to droplet fusion and expedite the evaporation of the droplets. Moreover, the use of a collection chamber restricts producibility due to the confined dimensions of the chamber, hindering the scalability of the system.

In response to the challenges mentioned previously, our prior research focused on the development of core–shell particles called liquid beads engineered to encapsulate the PCR mixture. In that study, we systematically evaluated the mechanical and thermal properties of liquid beads. Our findings revealed that liquid beads exhibited significant mechanical resilience under external pressure. Liquid beads with various shell thickness-to-radius ratios withstood horizontal forces exceeding 10 mN. Thermal stability tests demonstrated that liquid beads remained structurally intact at temperatures exceeding 100 °C, indicating their robustness for LAMP processes. Moreover, X-ray imaging provided confirmation of their smooth, spherical morphology, further substantiating their potential applicability for microfluidic nucleic acid amplification.[27] In a separate study, we demonstrated the cryostability of these liquid beads, confirming their structural integrity and functionality after freezing.[26]

Building on our previous findings, the current study explores the application of liquid beads for digital LAMP. We aim to assess the system's efficiency and reliability in producing high-throughput, uniform partitions, as well as its capability to maintain bead integrity and stability throughout the amplification process. The chosen target for quantitative detection is the gene cluster XALB1. We employed five serially diluted concentrations of target DNA, ranging from 7.2×10^{-6} to 0.18×10^{-6} ng μL^{-1}, to assess the sensitivity and linearity of the analysis. The negative reference comprised a mixture without the target. Each experiment was replicated three times to ensure robustness. As depicted in **Figure 2**, the particles containing the target molecules exhibited a distinct fluorescence signal, indicating the successful amplification of the target within the particles. The partitioned particles can be categorized into two groups: negative particles, which do not contain a target template, and positive particles, which carry the template. A threshold was set based on the highest relative fluorescent intensity observed among particles without any template. Particles were considered positive if their fluorescence intensity exceeded this threshold. Given the possibility of more than one target DNA being entrapped in the core, we employed a Poisson distribution model to quantify DNA for each sample, as presented in the following.

$$C = -\ln(1 - (d/n))/V \quad (1)$$

Here, d represents the number of positive particles, n indicates the number of particles detected, and V denotes the volume of the core droplet. The average volume of the core droplets was ≈0.17 nL. Figure 2 clearly illustrates a linear increase in the number of positive particles with rising concentration of target

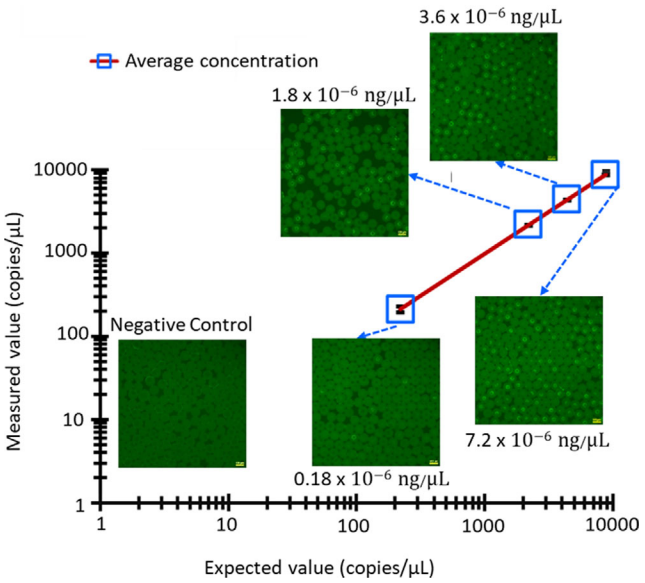

Figure 2. The measured DNA concentration encapsulated within liquid beads after amplification is plotted against the expected concentration values on a logarithmic scale. The graph is accompanied by fluorescent images of liquid beads, both without DNA (negative control) and containing serial dilutions of DNA at concentrations of 0.18×10^{-6}, 1.8×10^{-6}, 3.6×10^{-6}, and 7.2×10^{-6} ng μL^{-1} (*P* value of 0.989). Each experiment was conducted in triplicate for every concentration. Scale bars are 100 μm.

DNA. The linear regression equation was determined, revealing a high correlation coefficient ($R^2 = 0.99$), indicating a strong linear relationship between the measured and expected values (*P* value of 0.989). The solid shell effectively prevented droplet coalescence and inhibited the evaporation of the reaction mixture throughout thermal cycling. This can be explained by the hydrophobic nature of TMPTMA, a monomer with methacrylate groups containing nonpolar hydrocarbon chains. This hydrophobicity makes TMPTMA-based polymers resistant to water. Additionally, TMPTMA's multiple reactive sites allow for extensive crosslinking, leading to dense, rigid structures with low permeability.[28,29] As a result, enzymes and other large biomolecules generally cannot penetrate the tightly crosslinked polymer network. This innovative approach eliminates the need for designing a collection chamber, allowing seamless transferability to various containers without limitations.

Before conducting dLAMP with single droplets, our initial emphasis was on ensuring the generation of stable droplets. This involved the optimization of surfactant concentration in both the continuous phase and the collection container. Various formulations were tested, including mineral oil with 1% and 2% span 80, 2% span 80 combined with 1% Triton X, and 2% span 80 combined with 2% Triton X. The most promising results were achieved with a 2% span 80 concentration in the continuous phase. The addition of Triton X to the continuous phase led to the dissolution and disappearance of the generated droplets within the collection container. While droplets demonstrated sufficient stability at a 2% span 80 concentration within the microfluidic devices and immediately after collection, they exhibited a tendency to merge postheating. Consequently, we increased the span 80 concentration to 3% and 4%, and 5% in the collection container. We observed a significant reduction in droplet coalescence postheating at the 4% concentration. Beyond this concentration, no significant effects were noted. However, some droplets diminished in size due to reagent evaporation. We excluded such droplets by setting a specific threshold based on droplet size. Initially, we collected the droplets in a PCR tube, but during the transfer to a plate for microscopic examination, we experienced a substantial loss. Consequently, we directly collected the droplets in a plate. The mean volume of single droplets was 0.11 nL. DNA quantification was conducted using Poisson statistics. Consistent trends were observed in the results of dLAMP using single droplets and liquid beads. In **Figure 3**, it is evident that with DNA dilution, the number of positive droplets decreased. Significantly, a strong correlation was observed between the expected and counted values (*P* value of 0.992), affirming the reliability of the experimental outcomes. There was also no significant difference in the copy number of the target DNA detected by these two LAMP techniques (*P* value of 0.998).

In a separate study, our team developed a novel colorimetric detection system to improve the performance of a conventional LAMP assay.[30] The device integrates a PDMS microreactor block with embedded heating elements optimized for precise thermal control. Negative temperature coefficient thermistors were positioned under each reaction chamber to continuously monitor temperature, while an Arduino Uno microcontroller managed both the heating system and experimental timing. The integration of a high-precision RGB sensor further enables real-time colorimetric analysis. This setup allows quantification of the target DNA concentration by analyzing the time required for the color change to reach a specific threshold during the reaction. The device was validated using *Leifsonia xyli subsp. xyli*, a

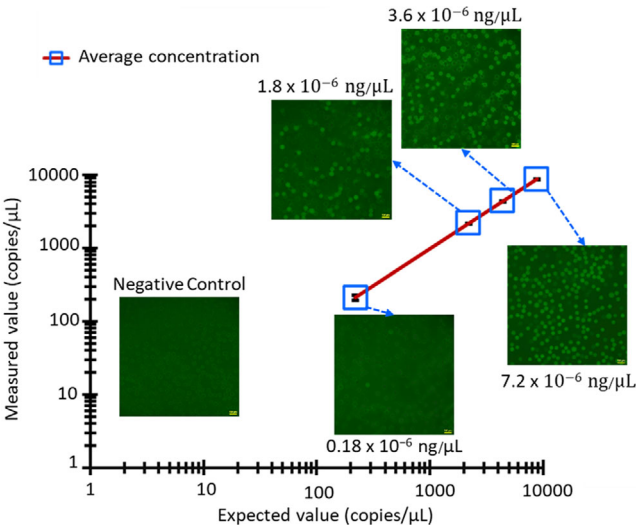

Figure 3. The DNA concentrations encapsulated within single droplets are compared to the expected values on a logarithmic scale. The graph includes fluorescent images of droplets without DNA and those containing serial dilutions of DNA at concentrations of 0.18×10^{-6}, 1.8×10^{-6}, 3.6×10^{-6}, and 7.2×10^{-6} ng μL^{-1} (*P* value of 0.992). Each experiment was conducted in triplicate for every concentration. Scale bars are 100 μm.

major pathogen causing ratoon stunting disease in sugarcane. The system demonstrated reliable tracking of dynamic color variations, allowing real-time monitoring of LAMP amplification that corresponded to the presence and concentration of the pathogen. In the team's recent work, the device was used to investigate the bacterial pathogen *Xalb*. The study revealed that at concentrations of 10^2, 10^3, and 10^4 cells per microlitre, the average detection times were 18.2, 16.7, and 14.9 min, respectively, showing a strong linear relationship ($R^2 = 0.8467$) between pathogen concentration and detection time. Extensive work with further details has been conducted and will be published soon, further demonstrating the device's potential for Xalb diagnostics and analysis.

When comparing this real-time monitoring system with digital LAMP using liquid beads, there are distinct differences in their applications and reagent requirements. Digital LAMP can be performed with a minute amount of reagents. The liquid beads generated in our device are better suited for situations where LAMP needs to be conducted postprocessing, particularly after exposure to harsh conditions in the field. This makes our system ideal for situations where stability and robustness are critical.

3. Conclusions

In summary, we presented an innovative digital LAMP assay using microfluidic liquid beads. This approach enables the generation of an unlimited number of particles without being hindered by the geometry and size limitations of reservoirs or incubation chambers. The resulting particles are easily collectible and transferable to various containers. In this investigation, we successfully quantified the X-lab genotypes at five distinct concentrations, ranging from 7.2×10^{-6} to 0.18×10^{-6} ng μL^{-1} using the liquid bead-based digital LAMP. The results demonstrated a close alignment with the expected target numbers in each sample, showcasing a linear regression pattern with the dilution of template concentration. The comparison of the digital LAMP methods using liquid beads and single droplets clearly revealed the advantages of the core–shell particle technique as a great partitioning option. In the case of single droplets, we observed coalescence and evaporation during the heating phase. Significant droplet loss was observed during the transfer from the PCR tube. This advancement brings digital LAMP closer to practical applications, enhancing its adaptability for laboratory use, especially in situations requiring the detection and quantification of a large number of target templates.

4. Experimental Section

Fabrication of the Microfluidic Device: We employed a standard photolithography technique to fabricate the master mold. Initially, a carefully cleaned silicon wafer, devoid of any dust, underwent spin coating with a layer of SU-8 3035 using a spin coater (WS-650-23 Spin Coater). Subsequently, the coated wafer was patterned through exposure to UV light at a dosage of 250 mJ cm$^{2-1}$. The patterned mold then underwent a baking process at 65 °C for 1 min, followed by 95 °C for 5 min. Afterward, the patterns were developed using a developer liquid on a shaker for 10 min. Following this development step, the master mold was cleansed with acetone and isopropanol. After the completion of the master mold, we employed the soft lithography technique to fabricate a polydimethylsiloxane (PDMS) device. A mixture of PDMS and curing agent with a ratio of 10:1 was poured into the mold and then degassed in a desiccator. The mixture underwent a 2 h heating at 75 °C in an oven. Upon curing, the PDMS was carefully separated from the mold, and inlets and outlets were perforated using a biopsy puncher. For enhanced adhesion, the cleaned PDMS substrate and a glass slide underwent oxygen treatment in a plasma cleaner (PDC-32G-2, Harrick Plasma) at a pressure of 1.2 mbar for 2 min, followed by bonding them together.

Following the assembly of the device, the channels underwent surface modification. Two distinct types of surface modifications were employed to facilitate the generation of core–shell droplets and single droplets. In the case of core–shell droplet generation, a 1 wt% polyvinyl acetate (PVA) solution was injected into the hydrophilic channels for a duration of 10 min. The flow of PVA was specifically directed into the hydrophilic channels by introducing air into the hydrophobic channels at a controlled flow rate of 400 μL min^{-1}. Subsequently, after the removal of PVA from the channels, the device was exposed to a temperature of ≈100 °C for 15 min. This multistep process was repeated three times to ensure the desired level of hydrophilicity. For the hydrophobic treatment, Aquapel was injected into the hydrophobic channels for 5 min. The flow of Aquapel was confined to the hydrophobic channels through the injection of air at a flow rate of 800 μL min^{-1}. Finally, Aquapel was completely discharged from the device by using compressed air. In the case of single droplet generation, the device was heated for 15 min at ≈100 °C. Subsequently, the channels were loaded with Aquapel, and after an 8 min interval, Aquapel was thoroughly removed by air blowing.

Droplet Generation: The complete microfluidic system comprised an inverted microscope (Ti, Nikon, Japan), five microinjection pumps (NEM-B101-03 A, CETONI GmbH, Germany), a high-speed camera (Chronos, Fotodiox Pro Lens), blue light, and the microfluidic chip. The microfluidic chip contained channels with different sizes: a constriction with a width of 30 μm at the first junction, a width of 100 μm from the first junction to the spiral channel, and a width of 400 μm along the spiral channel. All channels had a consistent height of 120 μm. Feed solutions were introduced into the device using five syringe pumps and polyethylene medical tubing (inner diameter/outer diameter = 0.86/1.52 mm, Adtech Polymer Engineering Ltd), as depicted in Figure 1. For the generation of core–shell droplets, the core phase, consisting of a LAMP mixture, and the shell phase, incorporating Trimethylolpropane Trimethacrylate (TMPTMA), were introduced simultaneously at the first junction. A solution of 50% v/v glycerol and 10^{-3} mol L^{-1} Tween 20 was injected at the second junction as the continuous phase, and a similar solution was introduced at the third junction as a spacer fluid. Droplet formation was observed in real-time and recorded using the high-speed camera connected to the microscope (Nikon, Eclipse Ti). All generated droplets were collected in a PCR tube and promptly exposed to blue light with wavelengths of 450 and 495 nm for curing for 30 min to harden the shell. Previous research has shown that the absorbance of TMPTMA in the blue and green light regions (400–500 nm) is moderate, around 0.1, indicating a notable potential for polymerization. Beyond 500 nm, the absorbance drops significantly, remaining near zero across the rest of the visible light spectrum, making it suitable for optical detection.[31] Following this, the tubes were transferred to a standard PCR machine (Bio-Rad CFX Connect, NSW, Australia) and heated at 65 °C for 30 min. The resulting particles were then transferred into a petri dish for analysis and imaging under a fluorescent microscope (Eclipse Ti2, Nikon).

To produce single droplets, the LAMP mixture was injected at the first junction, while, from other inlets, the oil phase containing mineral oil and surfactant was introduced. Two different surfactants, span 80 and Triton X, were examined at concentrations of 1% and 2% span 80, and combinations of 2% span 80 with 1% Triton X, and 2% span 80 with 2% Triton X. The resulting droplets were collected in mineral oil containing 2%, 3%, 4%, and 5% wt span 80. Subsequently, the collection container was heated in a standard PCR machine (Bio-Rad CFX Connect, NSW, Australia) at 65 °C for 30 min. Following this, containers were gently transferred to the stage of the fluorescent microscope for capturing images. We then analyzed all the microscopic images using Python and ImageJ.

Table 1. Primer sequences used for RT-LAMP.

Primer	Sequence
Xalb_F3	GATCTCGCGTATTGCCAGG
Xalb_B3	CTTGTGCAGGAACCACATGC
Xalb_FIP	TCGCTAAGCTGCGCTACCG-GCGATCGATCTGCCCCT
Xalb_BIP	CCAGCCATGCACGCGACA-AGTGGAAAGCGGAATGGTCG
Xalb_LF	GGCAGCTCGAACAGCAT
Xalb_LB	CGATGTCATCCCCGCAAGC

Preparation of LAMP Mixture: For each experimental trial, we freshly prepared the LAMP mixture before introducing it into the device. The reaction volume of 25 µL consists of 12.5 µL master mix, 0.5 µL dye, 2.5 µL primer mix, 2 µL target, and 7.5 µL water. The primers were designed using the New England Biolabs primer design tool, specifically targeting a 200 bp region within the albicidin pathotoxin biosynthesis gene cluster XALB1 (GenBank accession no. AJ586576.1). This region corresponds to positions 43128 to 43327 in the *Xanthomonas albilineans* GPE PC73 complete genome. The primer sequences are detailed in **Table 1**. Prior to introducing the target, the mixture underwent vortexing to ensure thorough mixing. Subsequently, target sequences with concentrations of 0.18×10^{-6}, 1.8×10^{-6}, 3.6×10^{-6}, and 7.2×10^{-6} ng µL^{-1}, were added to the mixture.

Statistical Analysis: The *z*-scores for all concentrations across both techniques were calculated and fell within the range of −1 to 1, suggesting that the values are close to the mean. A *t*-test analysis was performed using Python, with all *p*-values calculated as two-sided, considering $p < 0.05$ as the threshold for statistical significance. This approach ensured a rigorous evaluation of the data, leading to reliable and robust findings that allowed for a comprehensive comparison of the LAMP techniques.

Acknowledgements

This research was funded by an Australian Research Council (ARC) Discovery Project (grant no. DP220100261) amd ARC Laureate Fellowship (grant no. FL230100023). This work was conducted at the Queensland node-Griffith of the Australian National Fabrication Facility, established under the National Collaborative Research Infrastructure Strategy for nano- and microfabrication.

Conflict of Interest

The authors declare no conflict of interest.

Author Contributions

Fariba Malekpour Galogahi: conceptualization, experiment, validation, and writing—original draft. Simon Strachan: experiment. **Ajeet Singh Yadav**: experiment. Helen Stratton: methodology and conceptualization. **Nam-Trung Nguyen**: conceptualization, writing—review and editing, and supervision.

Data Availability Statement

The data that support the findings of this study are available from the corresponding author upon reasonable request.

Keywords

digital loop-mediated isothermal amplification, digital microfluidics, disease diagnoses, droplet-based microfluidics, liquid beads

Received: March 18, 2024
Revised: August 21, 2024
Published online:

[1] Y.-D. Ma, K. Luo, W.-H. Chang, G.-B. Lee, *Lab Chip* **2018**, *18*, 296.
[2] L. Jiang, X. Lan, L. Ren, M. Yang, B. Wei, Y. Wang, *Micromachines* **2023**, *14*, 1077.
[3] J. A. Tomlinson, I. Barker, N. Boonham, *Appl. Environ. Microbiol.* **2007**, *73*, 4040.
[4] S. Lei, S. Chen, Q. Zhong, *Int. J. Biol. Macromol.* **2021**, *184*, 750.
[5] G. Verma, B. Raigond, S. Pathania, T. Kochhar, K. Naga, *Eur. J. Plant Pathol.* **2020**, *158*, 951.
[6] A. Ansari, F. M. Galogahi, G. Millar, F. Helfer, D. V. Thiel, S. Soukane, N. Ghaffour, *Desalination* **2023**, *546*, 116207.
[7] R. Viswanathan, N. Geetha, A. Anna Durai, P. T. Prathima, C. Appunu, B. Parameswari, K. Nithya, T. Ramasubramanian, A. Selvi, *Genomic Designing for Biotic Stress Resistant Technical Crops*, Springer, Berlin **2022**, pp. 337–439.
[8] P. Champoiseau, P. Rott, J.-H. Daugrois, *Plant Dis.* **2009**, *93*, 339.
[9] V. D. Dias, E. Fernandez, M. G. Cunha, I. Pieretti, M. Hincapie, P. Roumagnac, J. C. Comstock, P. Rott, *Trop. Plant Pathol.* **2018**, *43*, 351.
[10] V. D. Dias, R. C. Filho, É. C. Dianese, M. G. Cunha, *Científica* **2019**, *47*, 21.
[11] Y. Shi, J.-Y. Zhao, J.-R. Zhou, M. S. Ntambo, P.-Y. Xu, P. C. Rott, S.-J. Gao, *Plant Dis.* **2021**, *105*, 3451.
[12] A. S. Yadav, F. M. Galogahi, A. Vashi, C. H. Ooi, S. K. Rajan, N.-T. Nguyen, *Lab Chip* **2023**, *23*, 3353.
[13] H. Yuan, Y. Chao, H. C. Shum, *Small* **2020**, *16*, 1904469.
[14] N. Zhang, C. Yue, J. Liu, X. Zhan, Z. Cheng, C. Li, Y. Du, F. Tian, *Anal. Bioanal. Chem.* **2023**, *415*, 627.
[15] H. Wu, X. Cao, Y. Meng, D. Richards, J. Wu, Z. Ye, A. J. DeMello, *Biosens. Bioelectronics* **2022**, *211*, 114377.
[16] N. Rong, K. Chen, J. Shao, Q. Ouyang, C. Luo, *Anal. Chem.* **2023**, *95*, 7830.
[17] A. A. Kojabad, M. Farzanehpour, H. E. G. Galeh, R. Dorostkar, A. Jafarpour, M. Bolandian, M. M. Nodooshan, *J. Med. Virol.* **2021**, *93*, 4182.
[18] F. M. Galogahi, Y. Zhu, H. An, N.-T. Nguyen, *Microfluid. Nanofluidics* **2021**, *25*, 82.
[19] S.-H. Tan, S. M. S. Murshed, N.-T. Nguyen, T. N. Wong, L. Yobas, *J. Phys. D: Appl. Phys.* **2008**, *41*, 165501.
[20] S. M. S. Murshed, S. H. Tan, N. T. Nguyen, T. N. Wong, L. Yobas, *Microfluid. Nanofluidics* **2009**, *6*, 253.
[21] F. Tian, C. Liu, J. Deng, Z. Han, L. Zhang, Q. Chen, J. Sun, *Sci. China Chem.* **2020**, *63*, 1498.
[22] M. Ho, N. Sathishkumar, A. A. Sklavounos, J. Sun, I. Yang, K. P. Nichols, A. R. Wheeler, *Lab Chip* **2024**, *24*, 63.
[23] P. Kumaresan, C. J. Yang, S. A. Cronier, R. G. Blazej, R. A. Mathies, *Anal. Chem.* **2008**, *80*, 3522.
[24] Q. Zhu, Y. Xu, L. Qiu, C. Ma, B. Yu, Q. Song, W. Jin, Q. Jin, J. Liu, Y. Mu, *Lab Chip* **2017**, *17*, 1655.
[25] F. M. Galogahi, Y. Zhu, H. An, N.-T. Nguyen, *J. Sci.: Adv. Mater. Devices* **2020**, *5*, 417.
[26] F. M. Galogahi, M. Christie, A. S. Yadav, H. An, H. Stratton, N.-T. Nguyen, *Analyst* **2023**, *148*, 4064.
[27] F. M. Galogahi, A. Ansari, A. J. T. Teo, H. Cha, H. An, N. T. Nguyen, *Biomed. Microdevices* **2022**, *24*, 40.

[28] M. Teotia, A. Mittal, R. K. Soni, *Materials for Biomedical Engineering*, Elsevier, Amsterdam **2019**, pp. 57–103.
[29] H.-J. Tai, P.-C. Chiang, Synthesis and Characterization of Methacrylic acid-based Copolymers, **2023**.
[30] S. Strachan, M. Chakraborty, M. Sallam, S. A. Bhuiyan, R. Ford, N.-T. Nguyen, *Micromachines* **2023**, *14*, 2101.
[31] H. L. Van Der Laan, M. A. Burns, T. F. Scott, *ACS Macro Lett.* **2019**, *8*, 899.